ORIGINAL RESEARCH

Distinct trends of pulsatility found at the necks of ruptured and unruptured aneurysms

Jordan Patti, Fernando Viñuela, Aichi Chien

Division of Interventional Neuroradiology, David Geffen School of Medicine at UCLA, Los Angeles, California, USA

Correspondence to
Professor Aichi Chien, Division of Interventional Neuroradiology, David Geffen School of Medicine at UCLA, 10833 LeConte Ave, Box 951721, Los Angeles, CA 90095, USA; aichi@ucla.edu

Received 8 January 2013
Revised 23 January 2013
Accepted 28 January 2013

ABSTRACT

Background Aneurysm hemodynamics has been shown to be an important factor in aneurysm growth and rupture. Although pulsatility is essential for blood flow and vascular wall function, studies of pulsatile flow properties in brain aneurysm disease are limited.

Objective To investigate differences in pulsatility within a group of ruptured and unruptured aneurysms by implementing patient-specific pulsatile flow simulation.

Methods 41 of 311 internal carotid artery aneurysms were selected from an aneurysm database (29 unruptured and 12 ruptured) and used for patient-specific hemodynamic simulations of pulsatile flow. Flow pulsatility changes in ruptured and unruptured groups were analyzed by comparing different components of blood flow. Pulsatility index (PI) was used to quantify the pulsatility of blood flow in each group at the aneurysm neck, body, dome, and parent artery.

Results Within the parent artery, PI did not significantly differ between ruptured and unruptured groups (0.58). Within unruptured aneurysms, values of PI similar to that of the parent artery were found (0.61). Trends of significantly higher PI (1.99) were found within ruptured aneurysms ($p<0.001$). These differences were localized at the aneurysm neck, where PI in ruptured (1.93) and unruptured (0.59) aneurysms was significantly different ($p<0.001$).

Conclusions A trend towards a lower PI, similar to that in the parent artery, was found in unruptured aneurysms, while ruptured aneurysms followed a trend of higher pulsatility. The difference was significant at the aneurysm neck, indicating that pulsatility and this location may be important aspects of aneurysm rupture and a useful predictor of the risk of aneurysm rupture.

INTRODUCTION

Because of the severe morbidity associated with brain aneurysm rupture, identifying the risk of such rupture remains an important research area. With improvements in computational power, scientists can now perform patient-specific flow analyses to study the mechanism of aneurysm rupture and compare the hemodynamic patterns in ruptured and unruptured aneurysms.[1–4] Although hemodynamics has been shown to be an important factor in aneurysm growth and rupture, the characteristics of blood flow that differentiate ruptured and unruptured aneurysms, indicating the risk of rupture, remain undefined.

Research on aneurysm hemodynamics has identified maximum flow force on the vessel wall (wall shear stress) and flow impingement as important parameters associated with aneurysm rupture.[1–3] Although these hemodynamic properties are useful snapshots that capture instantaneous flow properties at the peak of systole, aneurysmal flow is complex and dynamic. Because aneurysmal flow changes throughout the cardiac cycle owing to pulsation and morphology, parameters focusing on a single time point may oversimplify the periodic flow changes within aneurysms which affect vessel wall function in the long term.[5] Therefore, in order to better understand the relationship between flow and aneurysm rupture, it may be beneficial to explicitly study how flow changes during each cardiac cycle.

Blood flow is pulsatile, and the pulsatility is essential to maintain vessel wall function and transport nutrients and oxygen throughout the body. The periodic variation in blood flow originates with cardiac contraction and propagates throughout the circulatory system. The characteristics of pulsatile flow in the vascular tree reflect vessel geometry and wall elasticity and have previously been used in the diagnosis of vascular diseases.[6–8] Although pulsatility is also known to be essential for cerebral circulation and cerebral function, studies of pulsatile properties in brain aneurysm disease are limited.[9–11]

Aneurysmal blood flow, like flow throughout the circulatory system, is affected by the pulsatile nature and changes over the cardiac cycle. Pulsatility index (PI), a parameter that quantifies the level of pulsatility, can be used to describe the periodic flow changes in the vascular system.[9 12–14] To date, PI has had only limited use in aneurysm research, in small studies of only a few aneurysms.[9 12 15] In this paper, we have implemented patient-specific pulsatile flow simulation to investigate differences in pulsatility within a group of ruptured and unruptured aneurysms.

MATERIALS AND METHODS

Case selection

In research approved by the institutional review board, 311 internal carotid artery (ICA) aneurysms which were treated in our center from 1990 to 2011 were reviewed for hemodynamic analysis. To minimize the hemodynamic variation caused by aneurysm location, 173 ICA aneurysms at the region of the ophthalmic artery, the location with the most cases of ruptured aneurysm in our database, were included in this study. Among the 173 aneurysms, 41 cases (29 unruptured and 12 ruptured) had sufficient image quality for flow analysis. Detailed information about the aneurysm cases included in this study is reported in table 1.

To cite: Patti J, Viñuela F, Chien A. *J NeuroIntervent Surg* Published Online First: [*please include* Day Month Year] doi:10.1136/neurintsurg-2013-010660

Table 1 Aneurysm cases at internal carotid artery-ophthalmic artery regions (n=41)

	Ruptured (n=12)	Unruptured (n=29)
Patient characteristics		
Mean age (years), mean (SD)	57.8 (14.3)	55.3 (13.1)
Female gender, n (%)	12 (100)	28 (96.6)
Hypertension, n (%)	3 (25.0)	12 (41.4)
Smoking, n (%)	5 (41.7)	9 (31.0)
Aneurysm characteristics		
Aneurysm size (mm), mean (SD)	11.75 (6.3)	8.53 (33.8)
Aneurysm neck size (mm), mean (SD)	4.47 (1.20)	4.38 (1.56)
Aneurysm shape		
Spherical, n (%)	2 (16.7)	12 (41.4)
Non-spherical, n (%)	10 (83.3)	17 (58.6)

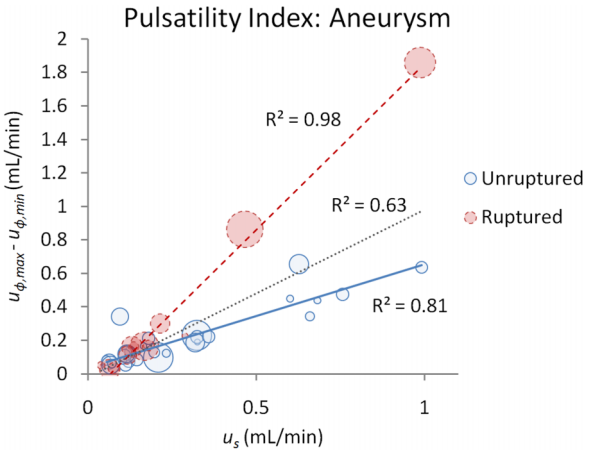

Figure 1 Plot of pulsatility within the aneurysm (neck, body, and dome combined). The x axis (u_s) corresponds to average flow rate, and the y axis ($u_{\varphi,max} - u_{\varphi,min}$) to the difference between maximum and minimum flow rate. The size of circles indicates the size of individual aneurysms, with circles in the legend ~8 mm diameter. Slope of lines corresponds to pulsatility index (Equation 2). Three linear regressions are shown, for ruptured (red, dashed), unruptured (blue, solid), and both groups of aneurysms combined (grey, dotted). R^2 values indicate quality of fit, with coefficients for the lines collected in table 2. Ruptured and unruptured aneurysms show distinctly different trends ($p<0.001$).

Pulsatile flow analysis

To study aneurysmal blood flow, three-dimensional (3D) angiograms acquired before aneurysm embolization procedures were used for the flow analysis (3DRA, Philip Medical System, Best, The Netherlands). Patient-specific aneurysm models were constructed based on 3D images of end-systolic shape and integrated into previously developed hemodynamic models which analyze the blood flow pattern based on incompressible Navier–Stokes equations.[3 4] The flow profile for each aneurysm was applied at the ICA of the simulation model based on an ICA flow profile acquired from a healthy volunteer using phase contrast magnetic resonance measurements as described in Cebral *et al*.[16] This standard flow profile provides a standard input PI and controls for additional acute differences between cases, allowing the study to focus on the hemodynamic effects resulting from ICA and aneurysm geometry.

Aneurysmal flow data were analyzed based on pulsatile flow changes over time (t). Because pulsatile flow is a combination of steady flow, $u_s(r)$, and oscillatory flow, $u_\varphi(r,t)$, where r is the radius of lumen size, the blood flow velocity can be expressed as Equation 1. Since PI is the ratio of the variation in flow velocity to the average flow velocity during a cardiac cycle, it can be expressed as Equation 2, which compares the steady and oscillatory component of blood flow within each aneurysm. In pulsatile flow conditions, the steady flow component is the average flow rate, and the oscillatory component captures the variation around that average. Therefore, when Equation 2 is applied, $u_{\varphi,max}$ is the maximum flow rate at any time during the cardiac cycle, $u_{\varphi,min}$, the minimum flow rate, andu_s, the average flow rate. Details of the equations for the flow analysis can be found in Zamir.[13]

$$\text{Pulsatile flow velocity } u(r,t) = u_s(r) + u_\varphi(r,t) \quad (1)$$

$$\text{Pulsatility index (PI)} = \frac{u_{\varphi,max} - u_{\varphi,min}}{u_s} \quad (2)$$

Statistical analysis

To compare the pulsatility in ruptured and unruptured cases, for each aneurysm, the average rate of blood flow (u_s, steady component) was plotted versus the variation in blood flow rate ($u_{\varphi,max} - u_{\varphi,min}$, pulsatile component) during the cardiac cycle. The method of least squares was used to calculate linear regressions for unruptured and ruptured groups of aneurysms. The regressions were then tested for coincidence by applying analysis of variance (F test) to compare fitting the two groups of data with separate regressions versus fitting all of the data with a single regression line. IBM SPSS 20 statistical software was used to perform the statistical analysis.

RESULTS

Linear regression analysis was applied to compare the ruptured and unruptured aneurysms at various locations within each aneurysm. Figure 1 shows the results for flow within the aneurysm sac. In this graph, as in the others, slope corresponds to PI. Additionally, the size of each aneurysm in figure 1 is denoted by the size of the circle. While ruptured aneurysms tend to be larger, no clear association between aneurysm size and PI was found. Figure 1 shows three linear regressions, for unruptured, ruptured, and combined aneurysm groups. Statistical comparison of the fit of ruptured and unruptured groups with separate regressions versus a single regression for both groups combined found that separate lines were a statistically significant improvement ($p<0.001$). This indicates two distinct trends for the ruptured and unruptured groups, with unruptured aneurysms tending to have lower PI than ruptured cases. The parameters for all linear regressions are summarized in table 2.

Detailed analysis of pulsatility for specific regions of aneurysms—aneurysm neck, body, and dome—is shown in figure 2. Regression lines were again calculated for ruptured and unruptured groups and compared with fitting both groups with a single line. In figure 2A, flow at the aneurysm neck mirrors the aggregate results for the aneurysm sac (figure 1). Separate regressions for ruptured and unruptured aneurysms provided a statistically better fit ($p<0.001$), showing that at the aneurysm neck ruptured and unruptured aneurysms had distinct differences in PI. The data in table 2 show that the neck fitting is better than the aneurysm sac as a whole. Figure 2B,C (body and dome) show no significant improvement in fitting two separate lines for ruptured and unruptured groups, indicating that at these locations PI is more broadly distributed and similar for

Table 2 Linear regression coefficients and fit (R^2) of oscillatory (variable) flow with respect to steady (average) flow

Location	Ruptured	Unruptured	Combined
Aneurysm (average) (p<0.001)	R^2=0.98	R^2=0.81	R^2=0.63
Slope (PI)	1.99	0.61	1.00
Intercept	−0.13	0.039	−0.021
Aneurysm neck (p<0.001)	R^2=0.98	R^2=0.90	R^2=0.66
Slope (PI)	1.93	0.59	1.055
Intercept	−0.14	0.069	−0.04
Aneurysm body	R^2=0.70	R^2=0.40	R^2=0.44
Slope (PI)	0.81	0.83	0.84
Intercept	0.042	0.054	0.050
Aneurysm dome	R^2=0.52	R^2=0.68	R^2=0.68
Slope (PI)	0.70	0.76	0.76
Intercept	0.063	0.056	0.056
Parent artery*	R^2=1.00	R^2=1.00	R^2=1.00
Slope (PI)	0.58	0.58	0.58
Intercept	0.11	0.18	0.17

*Excludes two outliers visible in figure 3.
PI, pulsatility index.

both groups. Therefore, the aneurysm neck appears to be the critical location when considering the pulsatility of blood flow and its differences between ruptured and unruptured groups.

Flow was also analyzed within the parent artery. These results are shown in figure 3. Results for the parent artery were different than within the aneurysm, and apart from two outliers, both ruptured and unruptured aneurysms varied little in PI, forming a nearly perfect line. Linear regression analysis found no statistically significant benefit to fitting separate lines for unruptured and ruptured groups (p>0.05). This finding is readily explained by the fact that all of the aneurysms share the same anatomical location. This further emphasizes that the difference in PI between ruptured and unruptured aneurysms shown in figures 1 and 2A arises from the unique geometrical characteristics of the aneurysms. Finally, while the flow rates were much higher in the parent artery than in the aneurysm sac (figures 1 and 3), in unruptured aneurysms, PI in the aneurysm sac (0.61) and at the aneurysm neck (0.59) was very close to PI in the parent artery (both ruptured and unruptured, 0.58) (table 2). In ruptured aneurysms, PI diverged greatly from the parent artery, with much higher values in the aneurysm sac (1.99) and neck (1.93) (figure 4).

DISCUSSION

In this study we investigated the pulsatility of aneurysmal flow and how pulsatility correlates with aneurysm rupture. The results indicate that for this sample of aneurysms from the same location, there are no significant differences in pulsatility at the parent artery between ruptured and unruptured aneurysms. However, significantly different trends were observed for ruptured and unruptured aneurysm sacs (figure 1), specifically at the neck of the aneurysms (figure 2A).

Exclusion of the aneurysm sac and neck from the circulation is a principle of aneurysm treatment, including surgical clipping and endovascular embolization devices. A neck remnant in treated aneurysms is known to present a risk of re-rupture and regrowth.[17 18] The underlying reason why complete occlusion of the aneurysm neck is so critical in treatment has never been clear. Through this quantitative study of a group of ruptured and unruptured aneurysms from the same location, we found a

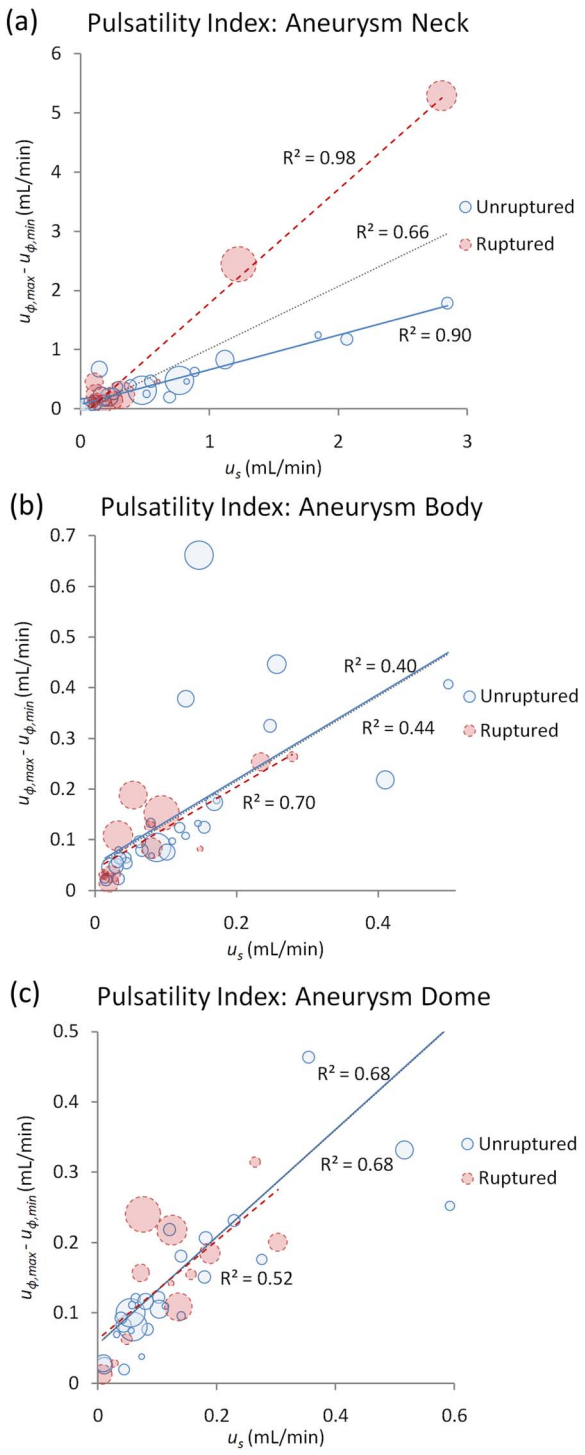

Figure 2 Variability in pulsatility at locations within the aneurysm. The x axis (u_s) corresponds to average flow rate, and the y axis ($u_{\varphi,max} - u_{\varphi,min}$) to the difference between maximum and minimum flow rate. The size of circles indicates the size of individual aneurysms, with circles in the legend ~8 mm diameter. Slope of lines corresponds to pulsatility index (Equation 2). Three linear regressions are shown, for ruptured (red, dashed), unruptured (blue, solid), and both groups of aneurysms combined (grey, dotted). R^2 values indicate quality of fit, with coefficients for the lines collected in table 2. (A) The aneurysm neck shows distinct trends of pulsatility index (PI) for ruptured and unruptured groups (p<0.001), as were found in the aneurysm as a whole. (B and C) The body and dome show no difference in PI between ruptured and unruptured aneurysm groups. While the fit (R^2) is poor for all groups at these two locations, the regressions show similar distributions for ruptured and unruptured groups.

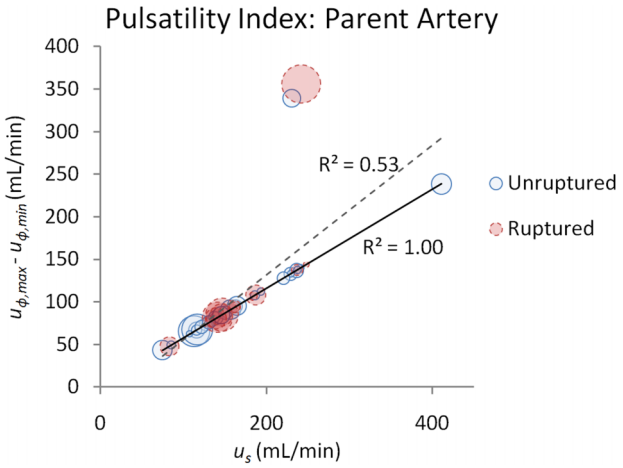

Figure 3 Variability in pulsatility in the parent artery. The x axis (u_s) corresponds to average flow rate, and the y axis ($u_{\varphi,max} - u_{\varphi,min}$) to the difference between maximum and minimum flow rate. The size of circles indicates the size of individual aneurysms, with circles in the legend ~8 mm diameter. Slope of lines corresponds to pulsatility index (Equation 2). R^2 values indicate quality of fit, with coefficients for the lines collected in table 2. Two linear regressions for pulsatility index (PI) are shown, the dashed line including all ruptured and unruptured aneurysms, and the solid line all aneurysms apart from the two outliers. Apart from the two outliers, all the aneurysms align with negligible variation in PI, illustrating that there is no statistical difference in pulsatility between ruptured and unruptured aneurysm groups at the parent artery ($p>0.05$).

trend of higher pulsatility at ruptured aneurysm necks, as well as a clear difference in pulsatility between the parent artery and the aneurysm site. Our data suggest that periodic flow changes at the aneurysm neck may be a key factor for aneurysm rupture. Consequently, when treatment successfully eliminates the flow stimulus to the aneurysm neck, it may interfere with the progression of aneurysm wall deterioration.

Overall, the results indicate that aneurysms with particular dynamic flow properties may be at higher risk of rupture. We found the same results when using linear regression to analyze coefficient of variation (data not shown), a similar metric to PI. Therefore, the relevant factor appears to be the variability in flow during the cardiac cycle. It should also be noted, that although rupture is often associated with larger aneurysm size, no clear association between aneurysm size and pulsatility was found.

This study illustrates the importance of considering flow changes throughout the cardiac cycle. Clearly, this type of analysis is not be possible without such data, and appears to be an important part of distinguishing between aneurysms that do and do not rupture (figure 4). Our data further suggest that it might be of value to develop interventional devices that reduce pulsatility at the aneurysm neck, based on designs which reduce the periodic changes of flow.

Geometrical characteristics that may help to discriminate unruptured and ruptured aneurysms have been studied extensively, but which are responsible for the variation in flow (PI) requires further research.[19 20] Interestingly, PI within unruptured aneurysms was similar to that in the parent artery. Given that variation in the amount of flow across the neck of the aneurysm was responsible for the difference between ruptured and unruptured aneurysms, further study combining pulsatility analysis and morphological characteristics of the aneurysm neck may be useful to help assess the rupture risks in incidentally found aneurysms. A future longitudinal study will consider how PI may change with treatment, and what relation, if any, this may have to aneurysm regrowth and re-rupture. Finally, more aneurysm cases from combined-center databases will be essential for future study to minimize bias due to case inclusion and further investigate the influence of pulsatility in aneurysms.

LIMITATIONS

The PI trend results presented in this paper are our findings from studying aneurysms at a single location (ICA-ophthalmic artery) from a single database. We selected this location to maximize the number of comparable ruptured cases, and it may reflect some bias in our database. Consequently, future studies incorporating more locations and additional databases will be necessary to determine the extent to which these PI trends apply to other aneurysm locations.

CONCLUSIONS

Blood flow pulsatility was quantified using PI, and its relationship with aneurysm rupture was analyzed. While both ruptured and unruptured aneurysms had similar pulsatility in the parent artery, the two groups showed distinctly different trends within the aneurysm, with ruptured aneurysms showing higher pulsatility. Differences in pulsatility between ruptured and unruptured

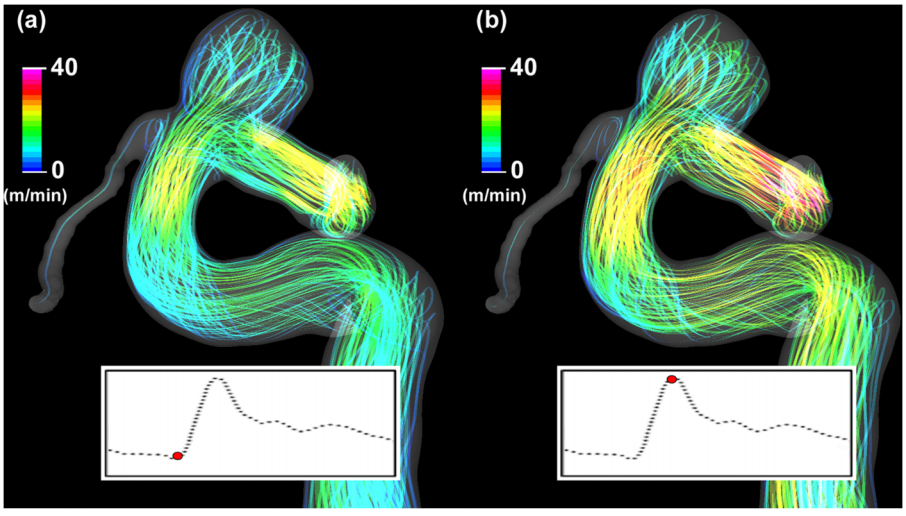

Figure 4 Streamline representation of (A) minimum and (B) maximum flow in a representative unruptured aneurysm. The color of streamlines indicates the rate of flow, showing how the pulsatile blood flow changes during the cardiac cycle, increasing in flow rate from (A) to (B). This is visible as a color shift towards yellow and red from (A) to (B).

aneurysms were particularly pronounced at the aneurysm neck, and may be an important factor for aneurysm rupture.

Contributors All the authors made substantial contributions to conception and design, acquisition of the data, or analysis and interpretation of data; drafting the article or revising it critically for important intellectual content; and final approval of the version to be submitted.

Funding This research is supported in part by a UCLA radiology exploratory research grant (#120003).

Competing interests None.

Ethics approval UCLA institutional review board.

Provenance and peer review Not commissioned; externally peer reviewed.

REFERENCES

1 Shojima M, Oshima M, Takagi K, *et al*. Magnitude and role of wall shear stress on cerebral aneurysm: computational fluid dynamic study of 20 middle cerebral artery aneurysms. *Stroke* 2004;35:2500–5.
2 Cebral JR, Castro MA, Burgess JE, *et al*. Characterization of cerebral aneurysms for assessing risk of rupture by using patient-specific computational hemodynamics models. *AJNR Am J Neuroradiol* 2005;26:2550–9.
3 Chien A, Tateshima S, Castro M, *et al*. Patient-specific flow analysis of brain aneurysms at a single location: comparison of hemodynamic characteristics in small aneurysms. *Med Biol Eng Comput* 2008;46:1113–20.
4 Chien A, Castro MA, Tateshima S, *et al*. Quantitative hemodynamic analysis of brain aneurysms at different locations. *AJNR Am J Neuroradiol* 2009;30:1507–12.
5 Safar ME, Levy BI, Struijker-Boudier H. Current perspectives on arterial stiffness and pulse pressure in hypertension and cardiovascular diseases. *Circulation* 2003;107:2864–9.
6 Romney JS, Lewanczuk RZ. Vascular compliance is reduced in the early stages of type 1 diabetes. *Diabetes Care* 2001;24:2102–6.
7 Agnew CE, McCann AJ, Lockhart CJ, *et al*. Comparison of rootMUSIC and discrete wavelet transform analysis of Doppler ultrasound blood flow waveforms to detect microvascular abnormalities in type I diabetes. *IEEE Trans Biomed Eng* 2011;58:861–7.
8 Westenberg JJ, Wasser MN, van der Geest RJ, *et al*. Variations in blood flow waveforms in stenotic renal arteries by 2D phase-contrast cine MRI. *J Magn Reson Imaging* 1998;8:590–7.
9 Benndorf G, Wellnhofer E, Lanksch W, *et al*. Intraaneurysmal flow: evaluation with Doppler guidewires. *AJNR Am J Neuroradiol* 1996;17:1333–7.
10 Lee YS, Yoon BW, Roh JK. Nonpulsatile cerebral perfusion in Takayasu's arteritis. *J Neuroimaging* 2003;13:169–71.
11 Kim YS, Chernyshev OY, Alexandrov AV. Nonpulsatile cerebral perfusion in patient with acute neurological deficits. *Stroke* 2006;37:1562–4.
12 Harders A. *Neurosurgical applications of transcranial Doppler sonography*. Wien; New York: Springer-Verlag; 1986.
13 Zamir M. *The physics of pulsatile flow*. New York: Springer; 2000.
14 Schubert T, Santini F, Stalder AF, *et al*. Dampening of blood-flow pulsatility along the carotid siphon: does form follow function? *AJNR Am J Neuroradiol* 2011;32:1107–12.
15 Le TB, Borazjani I, Sotiropoulos F. Pulsatile flow effects on the hemodynamics of intracranial aneurysms. *J Biomech Eng* 2010;132:111009.
16 Cebral JR, Castro MA, Soto O, *et al*. Blood-flow models of the circle of Willis from magnetic resonance data. *J Eng Math* 2003;47:369–86.
17 Guglielmi G, Vinuela F, Duckwiler G, *et al*. Endovascular treatment of posterior circulation aneurysms by electrothrombosis using electrically detachable coils. *J Neurosurg* 1992;77:515–24.
18 Fernandez Zubillaga A, Guglielmi G, Vinuela F, *et al*. Endovascular occlusion of intracranial aneurysms with electrically detachable coils: correlation of aneurysm neck size and treatment results. *AJNR Am J Neuroradiol* 1994;15:815–20.
19 Chien A, Sayre J, Vinuela F. Comparative morphological analysis of the geometry of ruptured and unruptured aneurysms. *Neurosurgery* 2011;69:349–56.
20 Raghavan ML, Ma B, Harbaugh RE. Quantified aneurysm shape and rupture risk. *J Neurosurg* 2005;102:355–62.